

# Numerical Evaluation of Quantum Efficiency in CdS/ZnSe Quantum Dot Solar Cells Using SCAPS and Quantum Disk Simulations

Rawaa Abbas Abd Ali<sup>1</sup>, Shymaa K. Hussian<sup>2,\*</sup>, Samir M. Abdula Mohsin<sup>1</sup> and Dheyaa A. Bilal<sup>1</sup>

<sup>1</sup> Department of Physics, College of Education for Pure Sciences, Thi-Qar University, Thi-Qar, 64001, Iraq

<sup>2</sup> Department of Physics, College of Science, Al-Muthanna University, Samawa, Iraq

Received: 2 Mar. 2025, Revised: 12 May 2025, Accepted: 2 Jun. 2025

Published online: 1 Sep. 2025

**Abstract:** This study numerically models and analyzes the quantum efficiency (QE) and absorption characteristics of CdS/ZnSe quantum dot (QD) solar cells using the Solar Cell Capacitance Simulator (SCAPS) and Quantum Disk theory. The investigation focuses on how variations in QD size, junction depth, and ZnSe layer thickness affect device performance. Results show that n-doped CdS QDs combined with p-doped ZnSe bulk layers enhance bandwidth and produce a QE peak within the ultraviolet range (240–330 nm). An optimal ZnSe layer thickness of 0.08  $\mu\text{m}$  yields a maximum efficiency of 13.5%. The findings offer design guidelines for improving thin-film photovoltaic devices based on QD architectures.

**Keywords:** Thin film Solar Cells, SCAPS, Quantum Dots, Quantum efficiency.

## 1 Introduction

Every year, the global demand for energy increases, while the availability of essential energy sources like fossil fuels continues to decline. As a result, various solar cell (SC) technologies are being actively researched and developed. Significant efforts are underway to produce third-generation solar cells, which involve using quantum dot nanostructures as light absorbers [1],[2]. Semiconductor quantum dots have attracted considerable interest due to their quantum-size effects [3]. These materials exhibit discrete energy levels and possess quantum characteristics similar to natural atoms or molecules [4].

Recently, significant interest has been directed toward semiconductor compounds due to their unique optoelectronic properties, such as a high absorption coefficient in the visible and infrared regions of the solar spectrum and a high efficiency of radiative recombination [5],[6]. Among these compounds, cadmium sulfide (CdS) stands out. CdS is a yellow-colored chemical compound with the formula CdS and functions as an electrical semiconductor. It exists in two distinct polymorphs: cubic hawleyite and hexagonal greenockite. CdS is chemically stable and has a narrow band gap of approximately 2.5 eV [7]. It also exhibits several remarkable physical properties, including strong mechanical strength, a high dielectric constant, and excellent insulating behavior, owing to its optical transmittance and high refractive index [8]. These characteristics make CdS an ideal material for various applications, particularly in photovoltaic devices and renewable energy systems [9].

On the other hand, zinc selenide (ZnSe), with a tunable

band gap, has been employed as a barrier layer in n-CdS/p-ZnSe heterojunctions [10]. ZnSe is an effective candidate for optoelectronic devices, as it covers a broad range of the visible and ultraviolet spectra, making it essential for high-performance optoelectronic applications [11]. The band gap of ZnSe alloys spans the solar spectrum from 2.8 eV (442 nm) to 5.6 eV (220 nm) [12]. Additionally, ZnSe exhibits excellent optical properties and has lattice constants closely matching those of ZnO [13].

Quantum efficiency (QE) is a crucial parameter in evaluating the performance of photovoltaic devices [14]. It quantifies how efficiently the incoming optical energy is converted into electrical current. An increase in efficiency is one of the key features that makes a solar cell (SC) more cost-effective [15]. In this study, the quantum efficiency QE and absorption coefficient were calculated for CdS/ZnSe QD SCs; the CdSQDs were n-doped, while the ZnSe bulk layer was p-doped, resulting in a wide bandwidth. It has been observed that the bandwidth increases as the disk height increases, but decreasing quantum efficiency QE (fewer) when increasing the disk radius decreases both quantum efficiency and the bandwidth. A high quantum efficiency can be achieved for CdS at a long depth of the structural junction of the solar cell.

## 2. Theory Section

### 2.1 Quantum efficiency QE in quantum dot Solar Cells

The continuity equation of minority carrier for holes in the p-side can be defined in Eq. (1) and for electrons in the n-side in Eq. (2)[16],

\*Corresponding author E-mail: [Shymaahussen@mu.edu.iq](mailto:Shymaahussen@mu.edu.iq)

$$D_p \frac{\partial^2 \delta p_n}{\partial x^2} - \frac{\delta p_n}{\tau_p} + G_L = 0 \quad (1)$$

$$D_n \frac{\partial^2 \delta n_p}{\partial x^2} - \frac{\delta n_p}{\tau_n} + G_n = 0 \quad (2)$$

Where the concentration of excess electrons (holes) that results from external excitation is defined as  $\delta p_n = p_n - p_{n0}$  ( $\delta n_p = n_p - n_{p0}$ ) with  $n_p(p_n)$  is the concentration of total electron (hole) at p-region (n-region) and  $n_{p0}(p_{n0})$  is the concentration of electron (hole) without an injection.  $\tau_n(\tau_p)$  is expressed as the lifetime of an electron (hole).  $D_n(D_p)$  is the electron (hole) diffusion coefficient. Also,  $G(x) = G_L$  in Eq. (1) is represented the steady-state generating rate, while the generation rate for the p-side is given by Eq.3 [17],

$$G_n = (1-R)\alpha_n\Phi \times \exp\{-(\alpha_n x_j + \alpha_d W + \alpha_p [x - x_j - W])\} \quad (3)$$

Where  $R$  represents the optical reflectance of a semiconductor and the air,  $\alpha(x)$  represents the coefficient of absorption of optical intensity (a function of the distance  $x$ ), and  $\Phi$  it's the number of illuminated photons.  $x_j, W$  are the depletion depth and width, respectively. Note that  $\alpha_n, \alpha_p$ , and  $\alpha_d$  are absorption coefficients of n-, p-, and depletion layers, respectively. In SCAPS-1D, the generation rate of electron-hole pairs due to light absorption is typically calculated based on the absorption profile of the materials and the illumination spectrum (like AM1.5G). It can be set in two main ways: This assumes a constant generation rate throughout the absorber layer.

Eqs. (1) and (2) are solved by summing particular and homogeneous solutions. Using some math calculations, we could derive the equation of hole density that is given by Eq.4 [18],

$$\begin{aligned} \delta p_n = & \frac{\alpha_n \phi (1-R) \tau_p}{(\alpha_n^2 L_p^2 - 1)} \left( \frac{\cosh(x/L_p)}{\sinh(x_j/L_p)} \right. \\ & \times \left[ -\frac{(D_p \alpha_n^2 - S_p)}{(D_p/L_p^2 - S_p)} e^{(x_j/L_p)} + e^{-\alpha_n x_j} \right] \\ & + \frac{(D_p \alpha_n^2 - S_p)}{(D_p/L_p^2 - S_p)} e^{(x/L_p)} - e^{-\alpha_n x} \end{aligned} \quad (4)$$

Where  $S_p$  is represents the velocity of surface recombination in the p-region. The diffusion-dominated hole diffusion photocurrent  $J_p$  nt at the n-side can be found using Eq.5 [16]

$$J_p \approx -q D_p \frac{\partial}{\partial x} \delta p_n \quad (5)$$

Thus, in the p-region, the equation for the electron diffusion photocurrent is Eq.6 [18],

$$\begin{aligned} J_n = & q \frac{\phi \alpha_p L_n (1-R)}{(\alpha_p^2 L_n^2 - 1)} e^{-(\alpha_n x_j + \alpha_d W)} \\ & \times \left[ \frac{(\alpha_p^2 - S_n) L_n^2}{(D_n - S_n L_n^2)} e^{-\alpha_p H'} \right. \\ & \left. - 2e^{-\frac{H'}{L_n}} + \alpha_p L_n e^{-\alpha_p H'} \right] \end{aligned} \quad (6)$$

The relation of drifting photocurrent  $J_{dr}$  from the depletion region can be described by Eq.7 [16],

$$J_{dr} = q \phi (1-R) e^{-\alpha_n x_j} (1 - e^{-\alpha_d W}) \quad (7)$$

And the QE equation is determined by Eq.8 [16],

$$QE = \frac{(J_p + J_n + J_{dr})}{q \phi (1-R)} \quad (8)$$

## 2.2 Boundary Condition Summary:

In this study, the quantum efficiency (QE) of CdS quantum dots (QDs) on ZnSe layers is modeled by treating the QDs as quantum disks with specific size ranges (12–14 nm in radius and 1–3 nm in height). The boundary conditions likely involve the spatial confinement of charge carriers within these QDs and the interaction at the interfaces between CdS and ZnSe layers. These constraints define the potential wells for electron and hole movement and are essential for solving the Schrödinger equation and simulating charge transport and optical absorption in the quantum dot solar cell structure.

## 2.3 Quantum Dots Solar Cell Structure

This research investigates quantum efficiency in CdS QDs produced on ZnSe layers. QEs are assumed to be represented as quantum disks with a range of sizes (radius of 12–14 nm and height of 1–3 nm). Fig.1 shows the graphical representation of different parts of the structure. Table 1 displays the CdS and ZnSe QDs' material parameters.

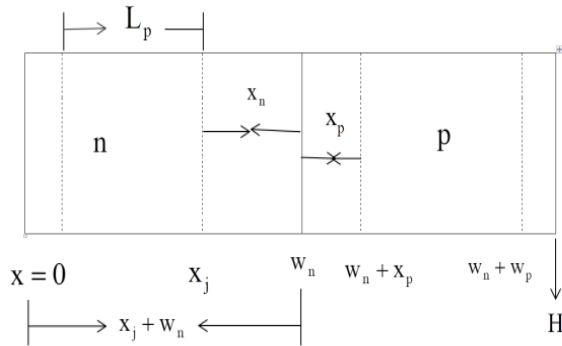


**Fig. 1:** A graphical representation of several layers in the structure of a QD solar cell. The n-type is 2  $\mu\text{m}$ , the p-type is 0.15  $\mu\text{m}$ .

**Table 1:** Material Parameters Used for CdS/ZnSe Quantum Dot Solar Cells in SCAPS Simulations.

Parameter	CdS (QD Layer)	ZnSe (Bulk Layer)	Units
Bandgap ( $E_g$ )	2.42	2.70	eV
Electron affinity	4.2	4.09	eV
Dielectric constant	10	9	-
Electron mobility(n)	100	200	$\text{cm}^2/\text{V} \cdot \text{s}$
Hole mobility (p)	25	50	$\text{cm}^2/\text{V} \cdot \text{s}$
Effective density of states (CB)	$2.2 \times 10^{18}$	$4.0 \times 10^{18}$	$\text{cm}^{-3}$
Effective density of states (VB)	$1.8 \times 10^{18}$	$3.0 \times 10^{18}$	$\text{cm}^{-3}$
Doping concentration (n-type)	$1 \times 10^{17}$	-	$\text{cm}^{-3}$
Doping concentration (p-type)	-	$1 \times 10^{17}$	$\text{cm}^{-3}$
Thickness	Variable (QDs: ~ 2nm)	0.02-0.15	$\mu\text{m}$
Absorption coefficient ( $\alpha$ )	$10^3 10^6$	$10^4 10^5$	$\text{cm}^{-1}$
Electron lifetime ( $\tau_n$ )	$10^{-9} - 10^{-8}$	$10^{-8}$	s
Hole Lifetime ( $\tau_p$ )	$10^{-9}$	$10^{-8}$	s
Surface recombination velocity (S)	$10^3 10^4$	$10^3$	$\text{cm/s}$

### 3. Results and Discussion

For CdS/ZnSe QD SCs structures at the sizes specified in section 2.2, QE was calculated using Eq. (8).

#### 3.1 Absorption spectrum of CdS/ZnSe Structure

The absorption spectrum of n-doped CdS/ZnSe quantum dot system when the disk radius ( $\rho = 13\text{nm}$ ) and the disk height ( $h = 2\text{nm}$ ) is shown in Fig. 2. As can be observed, it lies within the UV range of 240–340 nm

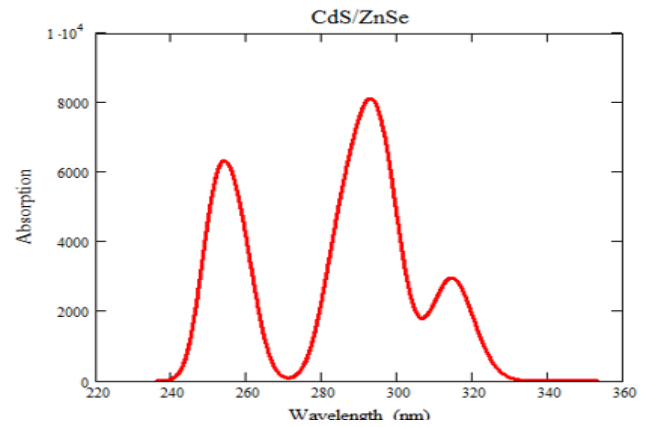


**Fig. 2:** shows the absorption spectrum for the CdS/ZnSe structure when  $h = 2\text{nm}$  and  $\rho = 13\text{nm}$ .

It can be detected that there are three peaks; The smallest one, which originates from the first subband transition, is located at 250 nm. The first ten subbands contribute to this first absorption peak collectively since they are close to one another. The second peak originates from the eleventh subband and is located at 290 nm. The ZnSe bulk p-doped region contributes as a QE at the p-doped QEp. The bulk region absorbed less light than the QD region. QE of CdS/ZnSe has a wide bandwidth where it can absorb wavelengths within the range of 240–330 nm. Another important feature that can be seen is the wide peak along all of this wavelength, which has not been obtained in any other structure of solar cell. Quantum efficiency was determined to be approximately 0.7.

#### 3.2 Quantum Efficiency against junction depth

This section includes a plot of QE against junction depth for various electron ( $L_n$ ) and hole ( $L_p$ ) diffusion lengths.

##### 1. Changing the Electron diffusion length $L_n$

Fig. 3 shows QE vs junction depth for the CdS/ZnSe QD structure at various electron diffusion length ranges. It is demonstrated that this material's electron diffusion length is effective, providing clear discrimination between QE Curves.

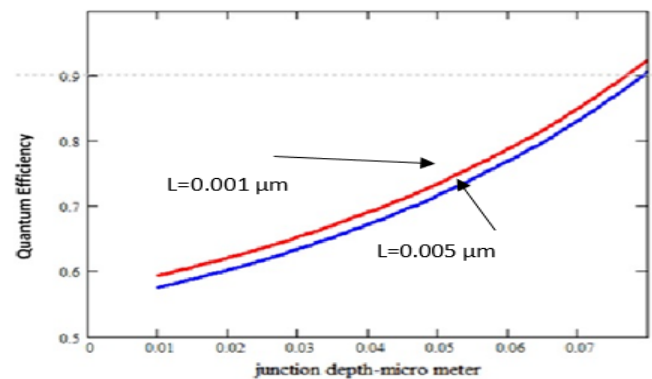


**Fig. 3:** Quantum efficiency of CdS/ZnSe QD structures at various values of the hole diffusion length  $L_n$ .

## 2. Changing the Hole diffusion length $L_p$

Fig. 4 shows quantum efficiency versus junction depth at various values of the hole diffusion length for the CdS/ZnSe QD structure. The hole diffusion length was efficient in this material and gave an obvious discrimination between QE Curves.

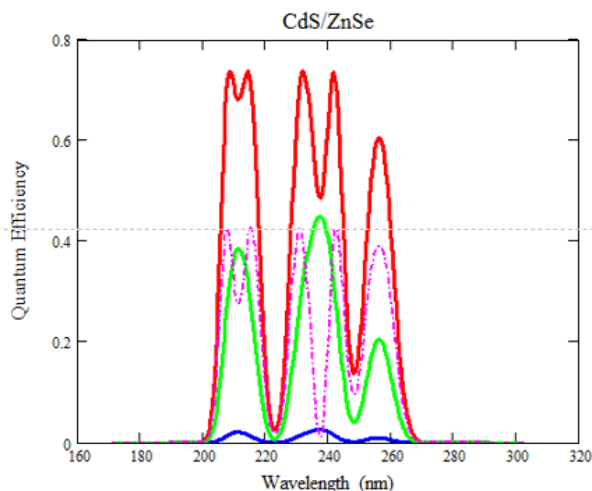


**Fig. 4:** The quantum efficiency CdS/ZnSe QD structure  $h=2\text{nm}$ ,  $\rho=13\text{nm}$ .

## 3.3 Impact of ZnSe layer thickness on solar cells

The effect of the thickness of ZnSe (n-type) on the planar solar cell, ranging from 0.02 to 0.15  $\mu\text{m}$ . Table 2 shows that as the thickness of the electron-transporting material is increased, FF, JSC, and system efficiency are increased until 0.8, where the efficiency reaches a maximum value of 13.5 %, then decreases. This means that the transmission of an incident photon (the solar cell characteristics) decreases as thickness increases, indicating that a thicker material offers a longer diffusion path for the electrons to reach the electrode, hence limiting the efficient charge collection.

**Table 2:** Variation of Thickness for ZnSe with Fill Factor and Efficiency

Thickness ZnSe ( $\mu\text{m}$ )	F.F(%)	$\eta$ (%)
0.02	21.06	12.65
0.04	21.02	12.24
0.05	20.95	12.8
0.06	20.87	12.9
0.07	20.80	13
0.08	20.74	13.5
0.09	20.68	10.51
0.100	20.62	9
0.110	20.57	8.5
0.120	20.53	7
0.130	20.48	6
0.140	20.44	6.2
0.150	20.41	6.2

## 4. Conclusion

This study demonstrates that optimizing quantum dot size, junction depth, and ZnSe thickness can significantly enhance the quantum efficiency of CdS/ZnSe QD solar cells. Maximum efficiency of 13.5% was obtained with a ZnSe thickness of 0.08  $\mu\text{m}$ . Future work should focus on experimental validation and explore defect passivation strategies to boost performance further.

## References

- [1] AbdulMohsin, S., J. Armstrong, and J. B. Cui. "CdS nanocrystal-sensitized solar cells with polyaniline as counter electrode." *Journal of Renewable and Sustainable Energy* 4.4 (2012).
- [2] R. Abbas Abd Ali, M. R. Al-bahrani, H.H. Waried," Design and Fabrication of TiO<sub>2</sub> \G Nanocomposite as Electron Transport Layer for Perovskite QD Solar Cells", *J Nanostruct* ,14(3),pp 953-962,(2024).
- [3] Hassan, Hadeer, Samir M. Abdulmuhsin, and Amin Habbe Al-Khursan. "Thallium quantum dot photodetectors." *Optical and Quantum Electronics* 52.2 (2020).
- [4] AbdulMohsin, S., J. Armstrong, and J. B. Cui. "CdS nanocrystal-sensitized solar cells with polyaniline as counter electrode." *Journal of Renewable and Sustainable Energy* 4.4 (2012).
- [5] Dakhil, Tahseen, Samir M. Abdulmuhsin, and Amin Habbe Al-Khursan. "Tunable mechanisms of quantum efficiencies in CdSe and TiO<sub>2</sub> quantum dot solar cells." *Applied optics* 57.4, 612-619, (2018).
- [6] Sh. K. Hussian, M. R. Al-bahrani," Investigation of the Characteristics of the Prepared TiO<sub>2</sub>/Graphene Films by Spin Coating Method", *J Nanostruct*, 14(1), pp. 168-175,(2024).
- [7] A.Abbasi and J. Jahanbin Sardroodi, "Modified N-doped TiO<sub>2</sub> anatase nanoparticle as an ideal O<sub>3</sub> gas sensor: Insights from density functional theory calculations", *Comput. Theor. Chem*, 1095, pp. 15–28,(2016).
- [8] Dakhil, T., S. M. Abdulmuhsin, and A. H. Al-Khursan. "Quantum efficiency of CdS quantum dot photodetectors." *Micro Nano Lett* 13.8, 1185-1187,(2018).
- [9] Al-Shatravi, Ali G., et al. "TiGaN quantum-dot photodetectors." *Semiconductors* 55.3, 359-362,(2021).
- [10] AbdulMohsin, Samir M., and Dhuha E. Tareq. "Fabrication and simulation of perovskite solar cells: A comparative study of CuO and Nano composite PANI/SWCNTS as HTM." *AIMS Energy* 8.2 (2020).
- [11] Sunaina, A.K. Ganguli, S.K. Mehta, "High

- performance ZnSe sensitized ZnO heterostructures for photo-detection applications", *Journal of Alloys and Compounds*, 894, pp. 162263, (2022).
- [12] A.Ohtomo, M.Kawasaki, T. Koida, K. Masubuchi, H. Koinuma, Y. Sakurai, and Y. Segawa, "Mg x Zn 1-x O as a II-VI widegap semiconductor alloy," *Applied Physics Letters*, 72, pp 2466-2468, (1998).
- [13] Sakban, Raunaq H., Mohammed D. Noori, and Samar M. Abdulmohsin. "Radical Enhancement Electric and Thermoelectric Efficiency of Graphene Nano Constrictions." *Solid State Technology* 63.1, 1788-1793, (2020).
- [14] B. Al-Nashy, S. M. M. Ameen and Amin H. Al-Khursan, "Kerr dispersion in a Y-configuration quantum dot system," *J. of Optics*, 16, p. 105205, (2014).
- [15] Tareq, Dhuha E., Samir M. AbdulMohsin, and Hussein H. Waried. "High Efficiency (41.85) of Br Perovskites base solar cells with ZnO and TiO2 comparable study as ETM." *IOP Conference Series: Materials Science and Engineering*. Vol. 928. No. 7. IOP Publishing, 2020.
- [16] Shin Mou, Jian V. Li, and Shun Lien Chuang, "Quantum Efficiency analysis of InAs-GaSb Type-II Superlattice Photodiodes", *IEEE J. Quantum Electronics*, 45, pp. 737-743, 2009.
- [17] AbdulAmohsin, S., Sabah Mohammed Mlkat al Mutoki, and M. Mohamed. "ZnO Nanowire/N719 dye/Polythiophene-SWNT nanocomposite solid state dye sensitized solar cells." *Autom. Control Intell. Syst* 3.2 (2015).
- [18] AbdulAmohsin, S. M., J. B. Cui, and M. Z. Mohammed. "Study on ZnO/p3HT: PCBM nanowire solar cells." *2013 IEEE 39th Photovoltaic Specialists Conference (PVSC)*. IEEE, 2013.